Supporting Information

Triple the capacity of optical vortices by nonlinear metasurface

Zhi Li[1], *Wenwei Liu*[1], *Zhancheng Li*[1], *Chengchun Tang*[2], *Hua Cheng*[1,4], *Junjie Li*[2], *Xianzhong Chen*[3], *Shuqi Chen*[1,4,*], *and Jianguo Tian*[1,4]

[1]The Key Laboratory of Weak Light Nonlinear Photonics, Ministry of Education, School of Physics and TEDA Institute of Applied Physics, Nankai University, Tianjin 300071, China.

[2]Beijing National Laboratory for Condensed Matter Physics, Institute of Physics, Chinese Academy of Sciences, P.O.Box 603, Beijing 100190, China.

[3]Institute of Photonics and Quantum Sciences, School of Engineering and Physical Sciences, Heriot-Watt University, Edinburgh, EH14 4AS, UK

[4]The collaborative Innovation Center of Extreme Optics, Shanxi University, Taiyuan, Shanxi 030006, China.

*Corresponding Author, email: schen@nankai.edu.cn

1. Set-up for measuring focal lengths and capturing optical vortices.

An LP and a QWP were combined to generate the incident circularly polarized light, the metasurface was illuminated at normal incidence and the generated linear and nonlinear optical vortices were filtered by another combination of a QWP and an LP, then collected with an objective, a tube lens and a scientific camera. The objective, tube lens and camera were all integrated on a XYZ translation stage to scan the focusing profiles of the optical vortices with a step of 1 μm along z-direction.

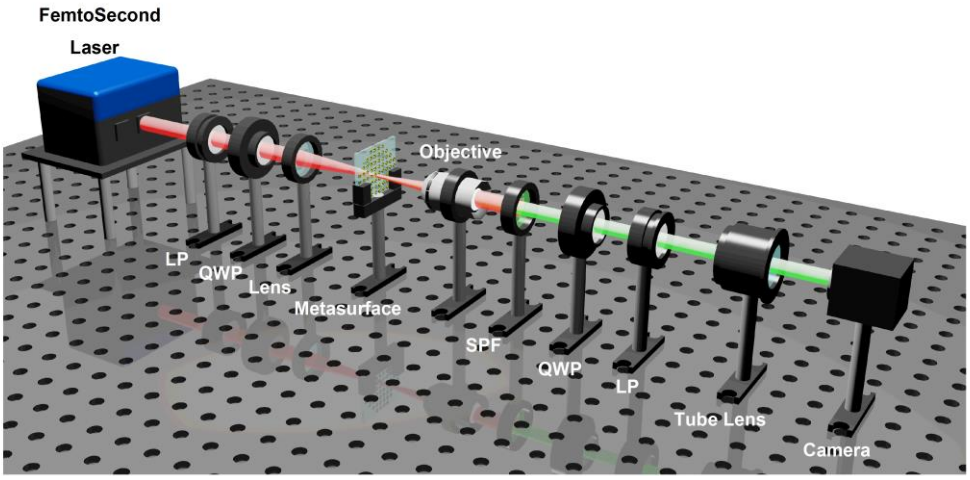

Figure S1. Illustration of the measurement set-up for measuring focal lengths and capturing optical vortices.

2. Analysis of the disturbance of period of the foci D.

As we have discussed in Equation (4) of the main text, the minimum period of the foci D is related to the period of meta-atoms Λ, and there should be a tolerance of Λ in the experiment. The disturbance in D of the linear focusing vortex can be calculated as:

$$\left|\frac{\Delta D}{D}\right| = \left|-\frac{\lambda f}{\Lambda^2}\cdot\frac{\Delta\Lambda}{D}\right| = 2.5\mu\mathrm{m}^{-1}\cdot\Delta\Lambda\,. \tag{S1}$$

The inner parameters (e.g. length and width) of the sample might be inaccurate in the fabrication process, but the period should be quite accurate as each meta-atom occupies the expected position.

The calculated disturbances $\Delta D/D$ of the linear and SHG optical vortices are all rather small as shown in Figure S2. The tolerance in Λ should be less than 5 nm in practice, thus the disturbance $\Delta D/D$ is less than 1.3%. With the same method, we then calculated the disturbances $\Delta D/D$ are less than 1.2% and 1.3% of the SHG focusing optical vortices with the same (σ) and opposite ($-\sigma$) circular polarization to that of the illumination light, respectively.

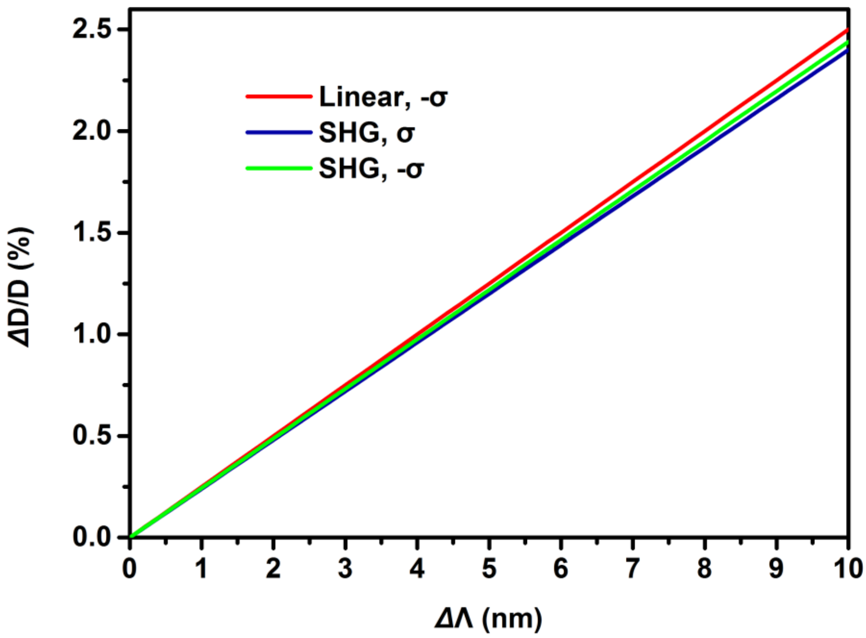

Figure S1. Calculated disturbances $\Delta D/D$ of the linear and SHG optical vortices as functions of tolerance in the period of meta-atom $\Delta\Lambda$.

3. Experimental demonstration of the THG focusing optical vortices.

Besides the SHG process, other nonlinear processes can also extend the capacity, such as the third harmonic generation (THG). As we discussed before, the nonlinear geometric phase of $2\sigma\theta$ and $4\sigma\theta$, new nonlinear focal lengths f_{n3} and f_{n4} can be introduced for THG signal with spin σ and $-\sigma$. Therefore two transmitted THG focusing optical vortices with $f_{n3} = 3\, f_0 = 90$ μm, $l_{n3} = 2$ (σ) and $f_{n4} = 3\, f_0/2 = 45$ μm, $l_{n4} = 4$ ($-\sigma$) can be generated, respectively. Measured intensity profiles along the propagation direction of THG focusing optical vortices with spin σ (Figure S3a) and $-\sigma$ (Figure S3c) indicate two nonlinear focal lengths f_{n3} about 88 μm and f_{n4} about 43 μm, which accord with the theoretical analysis. Besides, two-dimensional multifocal metalens has also been observed, based on equation (4), the theoretical distances between the foci of THG focusing optical vortices with spin σ and $-\sigma$ are 116 μm, and 59 μm, respectively, and the measured results shown in Figure S3b, S3d. For THG focusing optical vortices with spin $-\sigma$, the measured result is in agreement with the theoretical one, but it is hard to observe this phenomenon of the other spin due to the weak peak intensity far from the center. The topological charge of the THG optical vortex is hard to be quantified due to the weak signal intensity of the THG process.

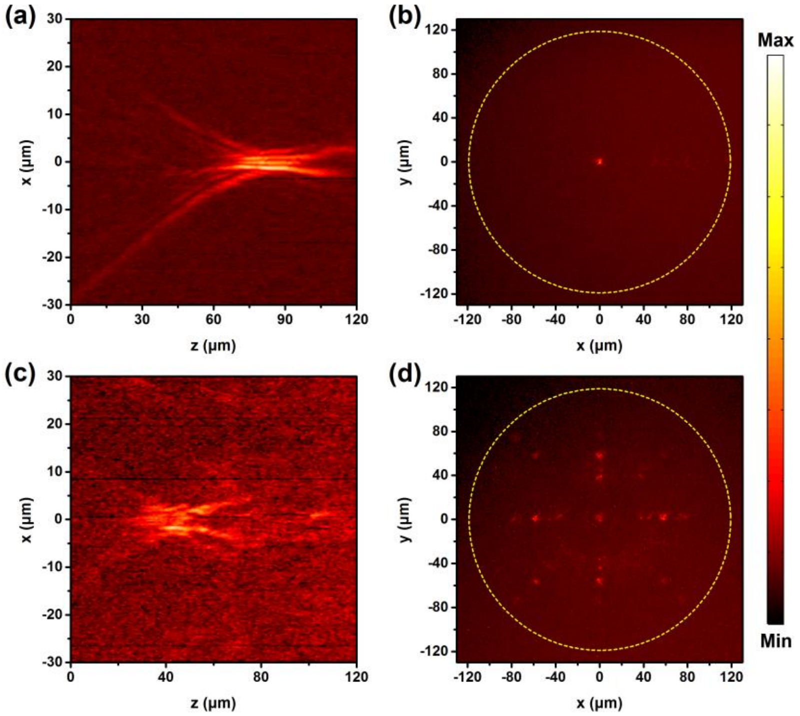

Figure S3. Measured intensity profile along the propagation direction (a) and intensity distribution at focal plane (b) of the THG optical vortex with spin σ. Measured intensity profile along the propagation direction (c) and intensity distribution at focal plane (d) of the THG optical vortex with spin -σ. The scale bar is adapted for each figure.

4. Numerical demonstration of the THG focusing optical vortices.

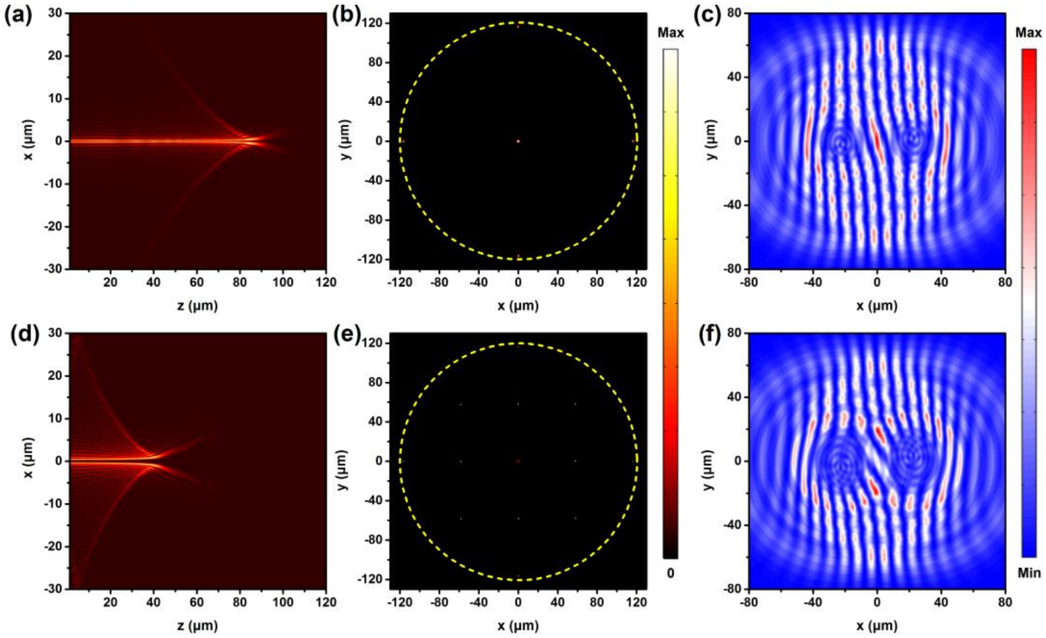

Figure S4. Numerical intensity profile (a), intensity distribution at focal plane (b) and self-interference pattern after the phase mask plane (c) of the THG optical vortex with spin *σ*. Numerical intensity profile (d), intensity distribution at focal plane (e) and self-interference pattern after the phase mask plane (f) of the THG optical vortex with spin -*σ*.

5. Simulated conversion efficiency of SHG.

Although the contributions of surface susceptibilities are larger than the bulk terms, they still behave "like bulk" when induced by the fast field variation at the metal interface [1]. Therefore, the effective bulk susceptibility 0.78 pm/V was used to simulate the SHG emission in gold nanoantennas [2]. In the simulation, the metasurface was illuminated with a normal-incident pulse with a field amplitude of 3×10^7 V/m for both the *x*- and *y*- components, corresponding to a peak intensity of 0.17 GW/cm^2 for circularly polarized light used in the experiment. The calculated total conversion efficiency is about 2

$\times 10^{-12}$, and the measured power rate of SHG with spin σ and $-\sigma$ is 1.45, thus the conversion efficiencies of SHG with spin σ and $-\sigma$ are about 1.65×10^{-12} and 1.14×10^{-12}, respectively.

References

[1] Butet J, Brevet P-F, Martin OJF. Optical second harmonic generation in plasmonic nanostructures: from fundamental principles to advanced applications. *ACS Nano* 2015; **9**: 10545-10562.

[2] Li Z, Liu WW, Li ZC, Cheng H, Chen SQ *et al*. Fano-resonance-based mode-matching hybrid metasurface for enhanced second-harmonic generation. *Opt. Lett.* 2017; **42**: 3117-3120.